Analysis on Non-stationary Characteristics of Wideband Radio Channel in HSR U-Shape Cutting Scenario

Lei Tian, Jianhua Zhang
Key Laboratory of Universal Wireless Communications (Beijing Univ. of Posts and Telecom.), Ministry of Education
Wireless Technology Innovation Institute, Beijing Univ. of Posts and Telecom., Beijing, 100876, China
E-mail tianlbupt@gmail.com, jhzhang@bupt.edu.cn

***Abstract*— High Speed Railway (HSR) wideband radio channel, as a vital fundamental prerequisite of the research on HSR communication technologies, attracts lots of attention with the tremendous development of HSR in China. The non-stationary characteristic of HSR radio channel caused by the high speed moving of the trains, has been considered as an important and hot research topic. In this paper, a metric of non-stationary characteristic of HSR channel is proposed referring to the theory of non-stationary random signal processing. At an aside, in order to solve the disunity of the index, the normalized non-stationary index is further defined. Then the non-stationary characteristic of HSR U-shape cutting scenario is analyzed by using the proposed metric based on the field wideband radio channel measurement data. The results show that the non-stationary degree of the HSR channel is severe when the varying rate of the Doppler is fast.**

I. INTRODUCTION

Recently, high speed railway (HSR) in China has made tremendous development after the great success in many other countries such as Germany, France and Japan, which has been a primary way for people travelling. As a result, the demand for high data rate and wideband communication services on HSR increases dramatically, which makes communication technologies for HSR attract more and more attention both in academic and industry.

The knowledge of HSR wideband radio channel, as a vital fundamental prerequisite of the research on communication technologies, has become an important topic. Channel measurement is the most direct and effective way to capture the channel characteristics. However, to the best of the authors' knowledge, most studies on HSR channel measurements are based on narrow-band measurements like the global system for mobile communications-railway (GSM-R). Only a few wideband HSR channel measurements are conducted over the world. A wideband HSR channel measurement campaign has been carried out at 5 GHz with 125 MHz bandwidth by using RUSK sounder of Medav in Germany [1]. Besides, two measurement campaigns were conducted at 2.35 GHz in the viaduct scenario of HSR by using Elektrobit PropsoundTM CS channel sounder [2] in Beijing and Taiwan of China, respectively [3], [4].

The HSR channel is considered to be quite different from the radio channel of traditional cellular network due to the extremely high travelling speed of the train. Various channel characteristics of HSR channel have been studied in most of the present literatures such as the large scale fading characteristics of HSR channel including path loss and K factor [5], [6], and delay characteristics and Doppler in the U-shape cutting scenario [7], [8]. However, there is rare work focusing on the non-stationary characteristics of HSR channel although most researchers consider the HSR channel could be non-stationary due to the high speed. Most present researches on non-stationary characteristics are for vehicle-to-vehicle (V2V) channel like [9] and [10]. For instance, [10] describes the non-stationary channel model of narrowband multiple-input and multiple-output V2V radio channel at 5.3 GHz based on the measurements. Therefore, in this paper, wideband channel measurements were conducted in the U-shape cutting scenario of Zhengzhou—Xian HSR line in China to investigate the non-stationary channel characteristics of HSR. And the non-stationary index is defined to interpret the degree of the non-stationary of the HSR channel.

The remainder of the paper is organized as follows. Firstly, the measurement equipment and environment are described in Section II. Subsequently, the pre-processing of the collected channel data and the method of the non-stationary index are explained in Section III. Then in Section IV, the results of the channel non-stationary characteristics are illustrated and discussed. Finally, conclusions are drawn in Section V.

II. MEASUREMENT EQUIPMENT AND ENVIRONMENT

The wideband radio channel measurement campaign was conducted along the Zhengzhou--Xian HSR line in China at the center frequency of 2.35 GHz with 50 MHz bandwidth by using Elektrobit PropsoundTM CS channel sounder. The clock signals of the transmitter (TX) and the receiver (RX) were precisely synchronized by the global position system (GPS) during the measurement campaign. A pseudo-random (PN) sequence of the code length of 127 chips was generated at the TX with a chip rate of 25 M chips/s and transmitted with the power of 33 dBm. At the RX, the channel impulse responses (CIRs) were obtained by slide correlating the received signal with a synchronized copy of the sequence at the channel samp-

(a) Vertical polarized dipole antenna (b) HUBER+SUHNER antenna

Fig. 1. Antennas used at (a) TX and (b) RX

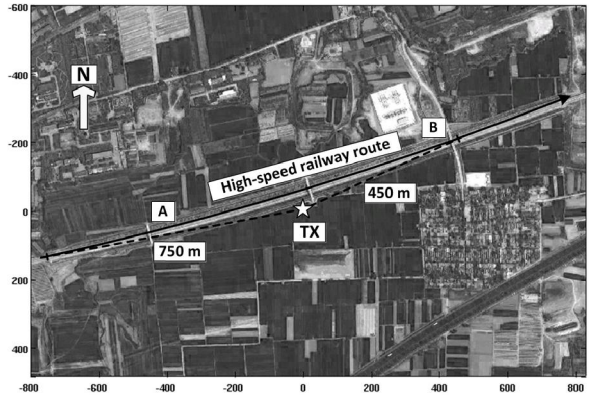

Fig. 2. Bird-eye view of measurement scenario. The star mark indicates the position of the TX. The solid arrow denotes the RX moving direction and route.

TABLE I. PARAMETERS OF MEASUREMENT CONFIGURATION

Item	Values
Center frequency	2350 MHz
Bandwidth	50 MHz
PN code length	127
Chip rate	25 Chips/s
Transmitting power	33 dBm
Channel Sampling Rate	1968.504 Hz

-ling rate of 1968.504 Hz. A vertical-polarized dipole antenna and a train-mounted wideband vertical-polarized antenna HUBER+SUHNER [11] were employed at the TX and RX, the outfit features of which are shown in Fig. 1. And the parameters of system configuration are summarized in Table 1.

The measurement scenario is illustrated in Fig. 2. The TX antenna marked by the star was fixed on a mast near the middle of the measurement route, which is 5 m high and about 20 m away from the U-shape cutting. The RX antenna was mounted on the high speed train moving at a constant speed of about 200 km/h in the U-shape cutting from the west to the east, shown as the black arrow in Fig. 2. The whole measurement route is approximately 1500 m long. A line-of-sight (LOS) path exists between the TX and the RX in most part of the route except for the part obstructed by the overpasses across the U-shape cutting. There are three overpasses on the route. One is close to the TX location. The other two are both about 450 meters away to the west and to the east of the TX location, respectively.

The upper width of the U-shape cutting is 40 meters, the bottom width is 16 meters, and the depth is 8.85 meters. It is a deep U-shape cutting according to the definition given in [5]. A broad plain with scattered scrubby trees extends along the U-shape cutting.

III. DATA PROCESSING

The data processing consists of two procedures: (1) pre-processing of wideband CIRs (2) calculation of channel non-stationary index.

A. Pre-processing of channel impulse responses

After the field wideband channel measurement, the CIRs are collected. The noise cutting is performed to obtain the pure CIR without the effect of the additive noise. Since the noise level P_{nl} of CIR varies during the measurement, the noise level is estimated for each CIR. Firstly, the valid CIRs are selected among the raw channel data. The CIR is considered to be valid if the power dynamic range which is calculated by $P_{\mathrm{dr}} = P_{\mathrm{p}} - P_{\mathrm{nl}}$ is larger than 25 dB, where P_{dr} is the power dynamic range, P_{p} is the peak power of the CIR. Then a threshold P_{th} is determined by $P_{\mathrm{th}} = P_{\mathrm{nl}} + D_{\mathrm{n}}$, where D_{n} is the noise margin from the noise level. The pure CIR consists of the multiple path components whose power is above the threshold P_{th}. In the data processing, D_{n} are set to be 6 dB.

The obtained pure CIR can be denoted as $h(t,\tau)$. For the purpose of eliminating the possible influence of correlated scatterers, $h(t,\tau)$ is firstly transformed to time-variant transfer function by doing Fourier Transformation over τ, i.e., $H(t,f) = \mathcal{F}_{\tau}\{h(t,\tau)\}$. Subsequently, $H(t,f)$ is divided over the frequency domain into N narrowband sub-channels, denoted as $H(t,i\Delta f), i = 1,\ldots N$ .Then the frequency response of each sub-channel can be calculated by

$$H(t,i\Delta f) = \frac{1}{\Delta f}\int_{f_c-\frac{B}{2}+(i-1)\Delta f}^{f_c-\frac{B}{2}+i\Delta f} H(t,f)\,\mathrm{d}f, \quad i = 1,\ldots,N, \quad (1)$$

where f_c and B denote the center frequency and the bandwidth, respectively.

B. Calculation of channel non-stationary index

Referring to the definition of the non-stationary index of non-stationary random signal, the channel non-stationary index

of each narrowband sub-channel can be defined based on the distance between the auto-correlation of the real time-variant transfer function and the estimated most closely wide sense stationary auto-correlation of time-variant transfer function.

Firstly, the time-variant transfer function of the ith sub-channel at time t_k is denoted as

$$H_k\left(t, i\Delta f\right), t \in \left(t_k, t_k + T\right), k = 1, \ldots K. \tag{2}$$

where T is the observation time duration, and K is the number of $H_k\left(t, i\Delta f\right)$. And the auto-correlation function can be calculated by

$$R\left(\mathrm{t}, \mathrm{s}; i\Delta f\right) = E\left[H\left(t; i\Delta f\right) H^*\left(t + s; i\Delta f\right)\right]. \tag{3}$$

In the sequel, the most closely wide sense stationary auto-correlation function is generally assumed to be the time average of all the K auto-correlation function, which can be expressed as

$$R_a\left(\mathrm{s}, i\Delta f\right) = \frac{1}{K}\sum_{k=1}^{K} R_k\left(\mathrm{s}, i\Delta f\right). \tag{4}$$

Finally, the channel non-stationary index is defined by the distance between the time-variant auto-correlation function and the time average auto-correlation function, which can be calculated by

$$S_k\left(i\Delta f\right) = \frac{\int\left[\left|R_k\left(\mathrm{s}, i\Delta f\right) - R_a\left(\mathrm{s}, i\Delta f\right)\right|^2\right]\mathrm{d}s}{\int\left|R_a\left(\mathrm{s}, i\Delta f\right)\right|^2 \mathrm{d}s}. \tag{5}$$

The zero value of $S_k\left(i\Delta f\right)$ indicates the channel is stationary whereas the non-zero value indicates the channel is non-stationary. The non-stationary degree of the channel is larger when the value of $S_k\left(i\Delta f\right)$ is larger. However, different selected T could lead to different results of $S_k\left(i\Delta f\right)$. Thereby, in order to eliminate the effect of different selected T, we calculate the normalized non-stationary index by

$$S_k'\left(i\Delta f\right) = \frac{S_k\left(i\Delta f\right)}{\max\limits_k\left\{S_k\left(i\Delta f\right)\right\}}, \tag{6}$$

where $\max\{\bullet\}$ denotes the maximum operation. The value range of $S_k'\left(i\Delta f\right)$ is $\left[0,1\right]$. If the channel is stationary, the value of $S_k'\left(i\Delta f\right)$ is zero. The value one of $S_k'\left(i\Delta f\right)$ indicates the maximum non-stationary degree of the channel.

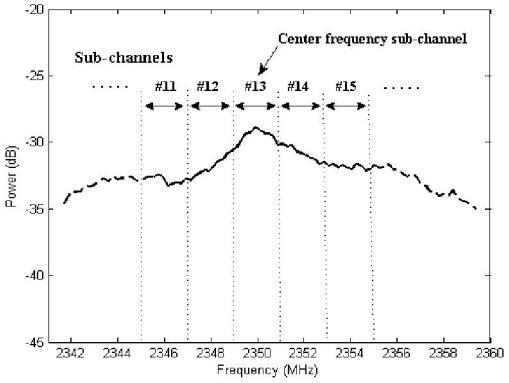

Fig. 3. Illustration of pre-processing of CIR.

IV. Results and Discussion

A. Overview of channel impulse responses

Although a large quantity of CIR samples is continuously collected, only the CIRs obtained between A and B marked in Fig. 2 are selected to be used in the following analysis of the non-stationary channel characteristics, since there is a good LOS propagation condition between TX and RX except for the area of the overpass near the TX.

As mentioned in the last section, the collected CIRs are firstly pre-processed by the noise cutting and frequency sub-channel division. For all the used CIRs, the power loss of the noise cutting is kept no more than 3% of the original power, which guaranteed the signal power is reserved to a large extent.

After the noise cutting, the CIR is transformed into the frequency domain and partitioned into narrowband sub-channels. The number of sub-channels is chosen to be 25 so that the bandwidth of each sub-channel is 2 MHz. Since the carrier frequency is 2350 MHz, the ratio of the sub-channel bandwidth to carrier frequency is 0.0008, which makes each sub-channel to be reasonably considered as a typical narrowband sub-channel. Fig. 3 illustrates the frequency response and sub-channel division of the CIR for the ease of understanding. The center frequency sub-channel is labeled by #13 in the figure.

B. Discussion on non-stationary index

The non-stationary index of all the sub-channels with $T = 50\dfrac{1}{f_s}$ is illustrated in Fig. 4. The horizontal axis indicates the time in the unit of second whereas the vertical axis indicates the sub-channel index. The zero point of the horizontal axis is the time corresponding to the location of A in Fig. 2. The brightness of the color represents the magnitude of the non-stationary index. Since the values of the non-stationary

index out of the time range where the figure shows are all nearly zero, only the results of the interesting time range corresponding to the area close to the TX is illustrated in the figure for simplicity. As the figure shows, the non-stationary indexes of different sub-channels are basically varying with the time in a similar way. Without the loss of generality, we inspect the varying of the center frequency sub-channel. It can be found that the channel shows severely non-stationary when the RX is travelling in the area around the TX. It accounts for that the non-stationary degree of the channel is somehow related to the variant rate of Doppler maximum frequency shift. The unexpected small values from 9.3 s to 9.6 s are caused by the weak signal reception due to the block of the overpass near the TX. It can also be seen in the figure that the non-stationary index decreases obviously at the sideband sub-channels, which is because of the non-ideality of the filter used in the measurement system. And the effective bandwidth is estimated to be about 40 MHz, which includes 20 sub-channels centered with the center frequency sub-channel.

In addition, we examine the influence of T to the non-stationary index. The average non-stationary index of the effective sub-channels is illustrated in Fig. 5 (a). The curves of different types indicates the non-stationary index results of different selected $T = 50\frac{1}{f_s}, 100\frac{1}{f_s}, \text{and } 150\frac{1}{f_s}$. As it is readily apparent in the figure, all the curves show a similar variation tendency versus the time. However, the absolute values are not the same. The bigger T is chosen, the larger the calculated value of the non-stationary index is.

Fig. 5 (b) shows the average normalized non-stationary index of the effective sub-channels. As the figure shows, the results of the normalized non-stationary index of different selected T are nearly the same. Comparing with the non-stationary index without normalization, the normalized index has two advantages. First, the value range of the normalized index is fixed from 0 to 1. Second, the value is not affected by T.

V. Conclusions

In this paper, we focus on the non-stationary characteristics of HSR channel in the U-shape cutting scenario. Referring to the non-stationary signal processing theory, a metric named the non-stationary index to evaluate the non-stationary degree of channel is proposed. Furthermore, the index is improved by doing a normalization operation in order to limit the value range to . Then, by using the defined non-stationary index, the non-stationary characteristics of the HSR wideband channel in the U-shape cutting scenario are analyzed based on the field measurement channel data. On one hand, it is found that the non-stationary degree of the channel is more severe when the Doppler frequency shift varies fast. On the other hand, the non-stationary degree of different narrowband sub-channels shows no significant differences. Moreover, we compare the non-stationary index with and without the normalization by using the measurement channel data, and verified the advantages of the improved non-stationary index.

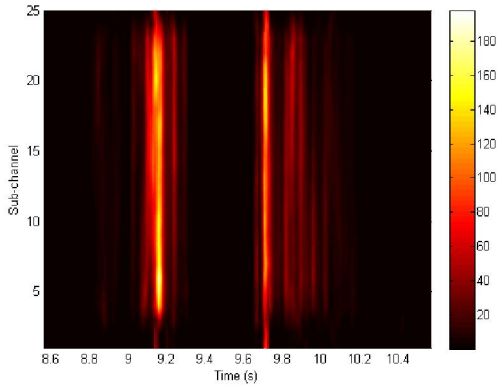

Fig. 4. Results of the non-stationary index with $T = 50 / f_s$ in the U-shape cutting scenario.

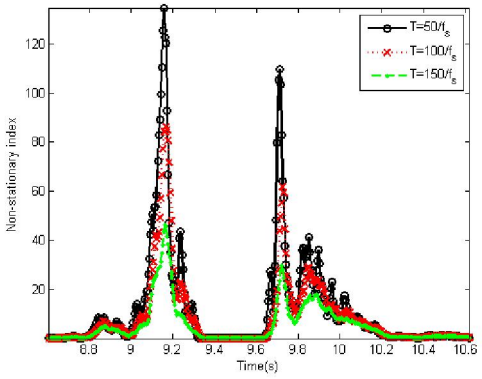

(a)Results without normalization

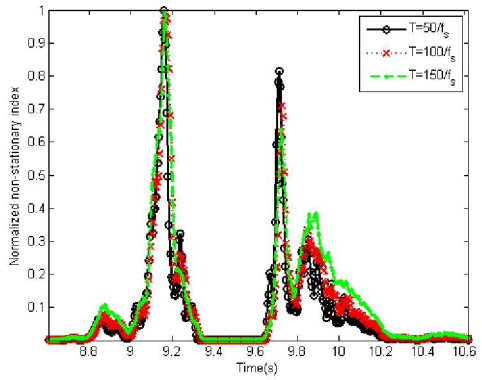

(b)Results with normalization

Fig. 5. Average non-stationary index of the effective sub-channels.

Acknowledgment

The research is supported by National Key Technology Research and Development Program of the Ministry of Science and Technology of China (NO. 2012BAF14B01), and National Science and Technology Major Project of the Ministry of

Science and Technology (NO. 2013ZX03003009), and National Natural Science Foundation of China (NO. 61171105), and Program for New Century Excellent Talents in University of Ministry of Education of China (NCET-11-0598).

REFERENCES

[1] WINNER II Channel Models, IST-WINNER II Deliverable 1.1.2, 2008.

[2] Propsound multidimensional channel sounder, Elektrobit Ltd. [Online]. Available: http://www.propsim.com.

[3] L. Liu, C. Tao, J. Qiu, H. Chen, et al., "Position-based modeling for wireless channel on high-speed railway under a viaduct at 2.35 ghz," IEEE J. Sel. Areas Commun, vol. 30, no. 4, pp. 834–845, 2012.

[4] R.Parviainen, K. Pekka, "Results of high speed train channel measurements," European Cooperation in the Field of Scientific and Technical Research, 2008.

[5] R. He, Z. Zhong, B. Ai, J. Ding, "Propagation measurements and analysis for high-speed railway cutting scenario," Electronics Letters, vol. 47, no. 21, pp. 1167–1168, 2011.

[6] J. Lu, G. Zhu, C. Briso-Rodriguez, "Fading characteristics in the railway terrain cuttings," Proc. IEEE 73rd Vehicular Technology Conference (VTC Spring), 2011.

[7] J. Qiu, C. Tao, L. Liu, and Z. Tan, "Broadband channel measurement for the high-speed railway based on wcdma," Proc. IEEE 75th Vehicular Technology Conf. (VTC'12 Spring), 2012.

[8] L. Tian, J. Zhang, C. Pan, "Small scale fading characteristics of wideband radio channel in the U-shape cutting of high-speed railway," Proc. IEEE 78th Vehicular Technology Conference (VTC'13 Fall), 2013.

[9] U. C. Okonkwo, S.Z.M. Hashim, R. Ngah, et al., "Time-scale domain characterization of nonstationary wideband vehicle-to-vehicle propagation channel," Proc. IEEE Asia-Pacific Conference on Apllied Electromagnetics (APAC 2010), 2010.

[10] O. Renaudin, V-M. Kolmonen, P. Vainikainen, C. Oestges, "Non-stationary narrowband MIMO inter-vehicle channel characterization in the 5-GHz band," IEEE Trans. On Vehicluar Technology, vol. 50, no.4, pp. 2007-2015, 2010.

[11] "Sencity rail antenna: 1399.17.0039 huber+suhner data sheet," HUBER+SUHNER AG RF Industrial, 2010.